

---

# TURBOFAN INTERACTION NOISE REDUCTION USING TRAILING EDGE BLOWING: NUMERICAL DESIGN AND ASSESSMENT AND COMPARISON WITH EXPERIMENTS

Cyril Polacsek, Raphaël Barrier

*ONERA, National Aerospace Research Agency, Châtillon, France*

Michael Kohlhaas, Thomas Carolus

*USI, Institute for Fluid and Thermodynamic, Siegen, Germany*

Philip Kausche, Antoine Moreau

*DLR, Berlin, Germany*

Fritz Kennepohl

*MTU Aero Engines, Munich, Germany*

*e-mail: [cyril.polacsek@onera.fr](mailto:cyril.polacsek@onera.fr)*

This paper investigates the effect of a flow control device on turbofan sound generation, applied to a low-speed axial compressor model in a laboratory test rig. This treatment consists in a secondary mass flow ejected through the trailing edge of the rotor blades, designed to fill the velocity defect behind the rotor and to decrease the turbulent kinetic energy related to the wakes, so that interaction noise should be reduced. The design and implementation of the blowing device is first briefly described, as well as the fan stage experiment. Then the paper focuses on computation methods devoted to the capture of turbulent wakes and to the acoustic response of the stator (with and without blowing). 3D steady RANS and quasi-2D LES approaches are considered for the CFD, both coupled to an integral formulation based on Amiet's theory aiming at calculating the in-duct sound power and estimating the acoustic performance of the treatment. Under optimal blowing conditions, significant sound power reductions are predicted by the simulations. First attempts to relate numerical predictions to available measurements, i.e. hot-wire data and in-duct sound power spectra, are proposed and discussed.

---

## 1. Introduction

A major source of broadband turbofan noise results from the interaction of turbulent rotor blade wakes with the outlet guide vanes (OGV). The objective of the present study is to assess the effect of a flow control device on sound generation, applied to a low-speed axial compressor model in a laboratory test rig, and studied in the framework of the European project FLOCON. This treatment consists in a secondary mass flow ejected through the trailing edge of the rotor blades (Trailing Edge Blowing, TEB). It is designed to fill the velocity defect behind the rotor and to decrease the turbulent kinetic energy related to the wakes, so that interaction noise should be reduced. Tone noise reduction has been successfully investigated by Brookfield<sup>1</sup> and Sutliff<sup>2</sup>, with optimal reduction around 10 dB. Further investigations of Sutliff et al.<sup>3</sup> focused on broadband noise, showing 2-3 dB maximum reduction due to turbulence decrease. However these results could not be confirmed by far-field measurements. An additional analysis is proposed here using extensive

numerical simulations and focusing on the broadband noise component.

The design and implementing of the blowing device performed by USI (University of Siegen), already detailed in a previous communication<sup>4</sup>, is first briefly described here, as well as the fan stage experiment. Then the paper focuses on computation methods devoted to the capture of turbulent wakes and to the acoustic broadband response of the stator (with and without blowing). 3D steady RANS and quasi-2D LES approaches are considered for the CFD, both coupled to an integral formulation based on Amiet's theory aiming at calculating the in-duct sound power and estimating the acoustic performance of the treatment. Although restricted to a thin radial extent, LES permits to locally assess the turbulence spectrum content and the integral length scale. These methodologies and the resulting blowing effect on turbulence characteristics and acoustic behavior are addressed. First attempts to relate numerical predictions to available measurements, i.e. hot-wire data and in-duct sound power level (SPL) spectra are discussed.

## 2. Fan stage model and trailing edge blowing implementation

The measurements were performed in a laboratory scale fan rig located at DLR Berlin. For the design and the implementation of the blowing devices a new fan with 18 blades containing internal passages for TEB was designed. Important design parameters are given in Table 1 and Fig. 1. Two x-hot-wire probes located downstream of the rotor trailing edge plane are used to measure the wake characteristics and a microphone rake provides the acoustic spectra in the outlet duct.

**Table 1.** Design parameters of the fan stage

Volume flow rate at the inlet $\dot{V}_{in}$	2.52	[m <sup>3</sup> /s]	Rotor speed, $N$	3159	[rpm]
Rotor diameter $D_A$	0.4524	[m]	Nr. of rotor blades, $B$	18	
Hub diameter $D_I$	0.286	[m]	Nr. of stator vanes, $V$	32	

For the rotor blade design, a NACA 6515-63 airfoil with span length  $L_{span} = 83.2$  mm is used. The fan operates at its design flow rate coefficient:

$$\phi_{in} \equiv \frac{\dot{V}_{in}}{\pi^2 D_A^3 N} = 0.21 \quad (1)$$

The position of the reference plane corresponds to the stator leading edge. The wake velocity profiles and the turbulent quantities are evaluated at a relative blade height of

$$h^* \equiv \frac{h}{(D_A - D_I)/2} \quad (2)$$

As the circumferential velocity and hence the flow velocity around the blade increases from hub to tip, the wake deficit increases as well. This requires a spanwise distribution of the blowing parameters. For that each blade slot is divided into five discrete orifices which are fed separately via internal passages. The optimal blowing angle is determined by the orifice geometry and the flow angle of the wake deficit.

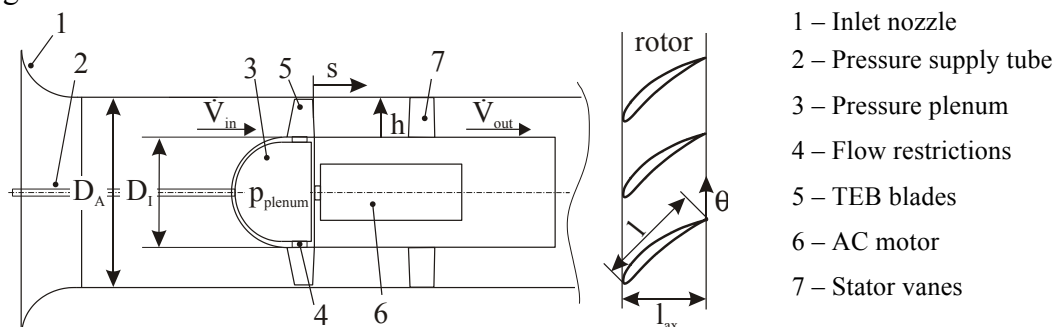


**Figure 1.** Schematic drawing of TEB fan stage: meridional cut (left) and coaxial section of cascade (right)

Fig. 2 shows the internal passages with guide vanes, shaped carefully to avoid excessive pressure losses. The internal passages responsible for a specific blade height are connected to the pressure plenum in the hub via flow restrictions which control the individual blowing mass flow rates. The inlet cross sections of the restrictions as well as the plenum pressure were optimized claiming a flat wake velocity profile. A pressure supply tube from the inlet nozzle to the plenum delivers the needed pressure as well as the overall TEB mass flow.

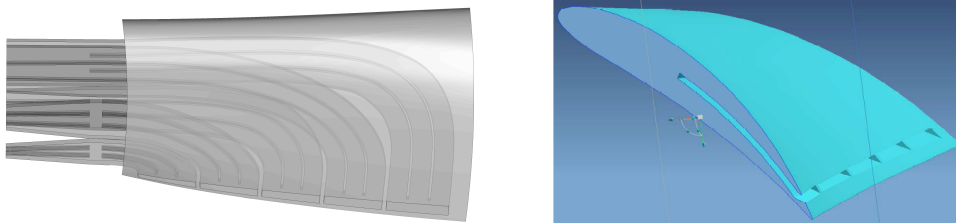


**Figure 2.** Rotor blade with internal passages, guide vanes and flow restrictors at the passage entrances (left), and CAD geometry (right) provided by USI

### 3. RANS-based and LES-based methodologies

#### 3.1 3D RANS computations (USI)

RANS computations are mainly performed by USI. The computational domain consists of 1/18th of the bladed annulus from  $1.0 D_A$  upstream to  $1.0 D_A$  downstream of the rotor. It also covers the five internal blade passages including the guide vanes from their inlet in the hub to their orifices where the jet flow mixes with the main flow. General grid interface (GGI) boundary conditions were imposed in the circumferential direction. The inlet mass flow rate of the fan system was imposed on the upstream boundary according to the operation point of  $\phi_{in} = 0.21$ , while an opening pressure boundary condition was set at the downstream boundary. At the entrance of each of the five internal blade passages the flow restrictions and the pressure plenum inside the hub were modeled. Of course no boundary conditions have to be specified at the channels exit (i.e. the orifices) since the flow mixes with the main flow. To solve the RANS equations, ANSYS CFX with the standard SST-turbulence model and a 2<sup>nd</sup> order approximation (blend factor of 1) was employed<sup>5</sup>. The block structured numerical grid consists of 7.1 million nodes. Special attention was paid to the wake region by using a very fine grid resolution of about 3 million nodes. Common grid quality criteria were considered in most of the fluid flow regions (grid angles  $> 20^\circ$ ). Due to geometrical restrictions, some grid angles in the TEB injection orifices were as small as  $13^\circ$ . In these regions, a finer grid was employed to ensure sufficient accuracy. For the simulation, the maximum value of  $y^+_{max}$  for the first node adjacent to the blade surface was  $< 6$ , whereas the area averaged  $y^+_{ave}$  at the blade was  $< 1$ . The convergence criteria were set to  $1 \cdot 10^{-6}$  MAX residuals.

#### 3.2 3D RANS and quasi-2D LES computations (Onera)

3D RANS computations have been also performed on baseline case using the CFD Onera code elsA that solves the compressible equations in the relative frame with a cell-centered finite volume formulation. Space discretization is ensured using Jameson's second-order-centered scheme with the addition of an artificial viscosity. Turbulence closure is achieved using the k-L turbulence model of Smith. The computation is performed on a single rotor passage using a multi-block grid of about 1 million nodes. A particular attention has been paid to the mesh downstream of the blade to keep a good description along the wake development zone. The mesh has 17 cells in the rotor tip gap. Exit plane is located approximately at 3 chord lengths from the rotor trailing edge.

Due to CPU and memory limitations, LES approach is practically restricted to a quasi-2D computation<sup>6,7</sup> so that the simulation is only focused here on a thin strip ( $L_{strip}$ ) of the full spanwise response. As done in Ref. 6, the sub-grid scale viscosity is given by the WALE model (Wall Adapting Local Eddy-viscosity)<sup>8</sup>. The quasi-2D computation domain is a cut in a circumferential plane at mid-span (corresponding precisely to half height of the central injection slit for the blowing

case), and extruded in spanwise direction over 20% of the chord (Fig. 3, left). The full 3D test-case is thus converted to a cascade-like test-case for the LES simulation, assuming that flow physics of the fan rig remains well captured by this conversion. The mesh size ( $\Delta x$ ,  $\Delta y$ ,  $\Delta z$ ) near the airfoil must verify some criteria for the validity of the LES computation. Non-dimensional criteria used for the present study are:  $\Delta x^+ \leq 40$ ,  $\Delta y^+ \leq 2$ ,  $\Delta z^+ \leq 20$ .

The blowing mass-flow in the central injection slit obtained from a 3D computation (USI) is translated in the quasi-2D LES as an equivalent mass-flow by using a uniform blowing along the whole extrusion of the blowing slit (Fig. 3, right). Optimal blowing conditions issued from USI computations were obtained with  $\dot{m}_{blowing} = 142$  g/s.

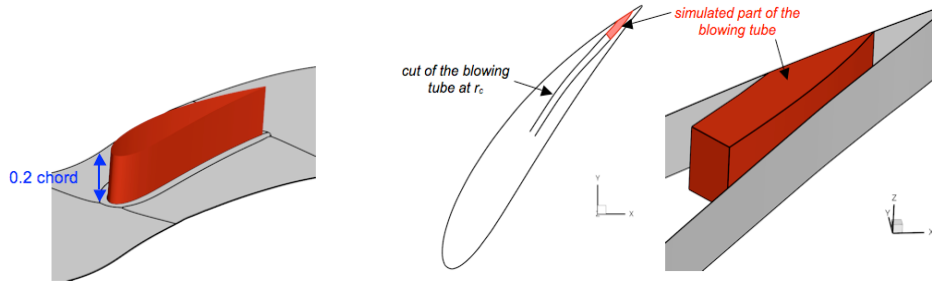


**Figure 3.** LES spanwise extrusion (left) and simulated part of the blowing tube (right)

### 3.3 Acoustic post-processing based on Amiet's broadband noise theory

This section presents the Amiet-based theory adopted here in order to predict broadband interaction noise, using either 3D RANS or 2D LES output data. A concise form of Onera formulation<sup>9</sup> providing the acoustic PSD ( $S_{ww}$ ) in the outlet duct can be written as:

$$S_{ww}(f) = V \sum_{m=-m_{\max}}^{+m_{\max}} \sum_{n=1}^{n_{\max}} \varphi_{mn}(r_s, f) |\mathcal{L}(r_s, K_c, 0)|^2 U_c \phi_{u_n u_n}(K_c, 0) \quad (3)$$

$\varphi_{mn}$  is a kernel function related to the Green's function (valid for an annular duct and a uniform mean flow),  $\mathcal{L}$  is the aeroacoustic transfer function obtained from the aerodynamic response of an isolated (zero-thickness) stator vane.  $K_c$  and  $U_c$  are respectively the convection wave-number and the convection speed, taken equal to the streamwise velocity ( $U_s$ ).  $\phi_{u_n u_n}$  is the 2-wavenumber turbulence spectrum related to the upwash velocity component,  $u_n$ , and adjusted using standard Von-Karman model.  $\phi_{u_n u_n}$  can be expressed versus the turbulent velocity spectrum,  $S_{u_n u_n}$ , and the spanwise correlation length scale,  $\ell_y$ :

$$\phi_{u_n u_n}(K_c, 0) = \frac{U_c}{\pi} S_{u_n u_n}(\omega) \ell_y(\omega) \quad (4)$$

$\phi_{u_n u_n}$  requires the knowledge of the mean-square turbulent velocity,  $u_{turb}$  (also related to the kinetic energy,  $k$ ), and the integral length scale,  $\Lambda$ . These information are usually obtained from a RANS calculation. In Eq. (4), upwash turbulent velocity spectrum and spanwise correlation length scale might be directly post-processed from LES output data, as done here for  $S_{u_n u_n}$ . However, assessment of  $\ell_y$  is practically not feasible, because the radial extent is too thin. An alternative approach is to use an analytical expression for  $\ell_y$  deduced from the Von-Karman spectrum and directly related to  $\Lambda$ , as discussed by Lynch<sup>10</sup>. CFD data extraction for RANS and LES output post-processing is sketched in Fig. 4. Inter-stage red plane in Fig. 4 (left) corresponds to the hot-wire position in the DLR rig. Inputs to Eq. (4) are taken at stator leading edge (LE) position. In Fig. 4 (right), LES data are interpolated from the rotating frame to the fixed frame and uniformly distributed along mean streamline assumed to represent the path of convected turbulent structures impacting the stator vane (chord aligned to this path). This allows us to calculate the turbulent velocity spectra and the integral length scale at mid span.

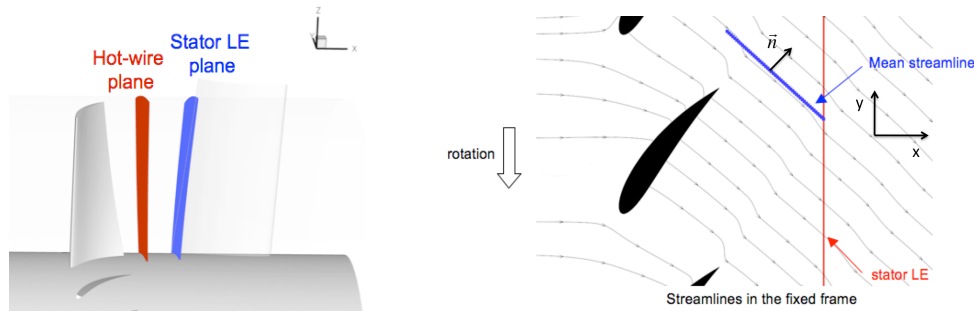


**Figure 4.** CFD data extraction for aeroacoustic analyses: 3D RANS (left) and quasi-2D LES (right)

## 4. Aerodynamic and noise predictions and comparison with experiment

### 4.1 Rotor wake characteristics

Firstly, wake characteristics in terms of velocity defect and turbulence intensity have been analyzed in order to check the reliability of the CFD computations (by comparison to the experiment on baseline case) and to estimate the effect of the blowing. Axial velocity profiles computed by USI RANS are compared to the measurements for two spanwise stations in Fig. 5. Predicted and measured blowing effects are similar, showing a significant reduction at 74% span but an overshoot at 44% span, revealing an inhomogeneous filling in the radial direction.

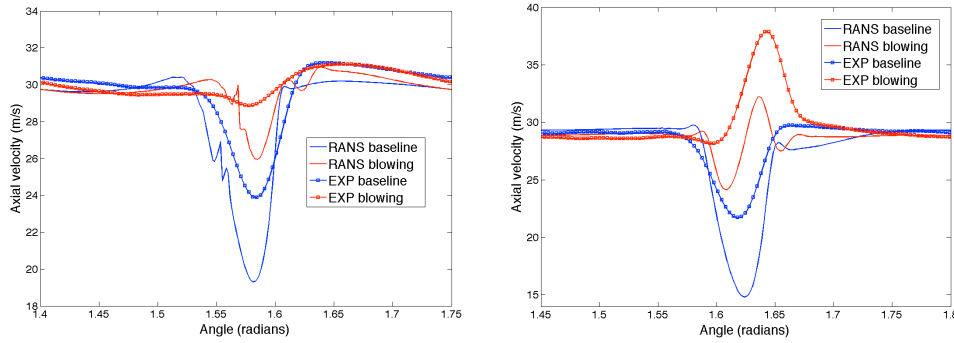


**Figure 5.** Axial velocity profiles issued from USI RANS and experiment at 74% (left) and 44% (right) span  
Turbulence intensity,  $T_u$ , scaled by axial, radial and tangential velocity components is defined as:

$$T_u = \frac{u_{turb}^{1/2}}{U_s} = \frac{u_{turb}^{1/2}}{\sqrt{U_x^2 + U_r^2 + U_t^2}} \quad ; \quad u_{turb} = \frac{1}{3} \left( \langle u_x^2 \rangle + \langle u_r^2 \rangle + \langle u_t^2 \rangle \right) = \frac{2}{3} k \quad (5)$$

$T_u$  360°-plots issued from USI RANS baseline computation (1 rotor blade channel) and from baseline and blowing experimental cases (18 blade passages) are compared in Fig. 6. Agreement between prediction and measurements is rather good, although the turbulent wake level is over estimated by RANS. Measured  $T_u$  wakes are clearly attenuated when the blowing is active (Fig. 6, right), despite of slight blade-to-blade irregularities. This effect is highlighted in Fig. 7 comparing the  $T_u$  plots over 1 blade channel (time-averaging using blade passing trigger in the experiment).

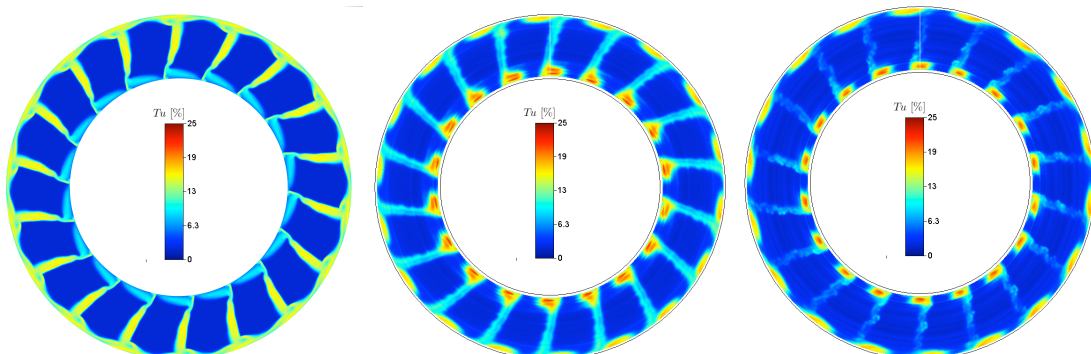


**Figure 6.** Turbulent intensity plots: RANS-SST (baseline, left) and exp. (baseline, mid. and blowing, right)

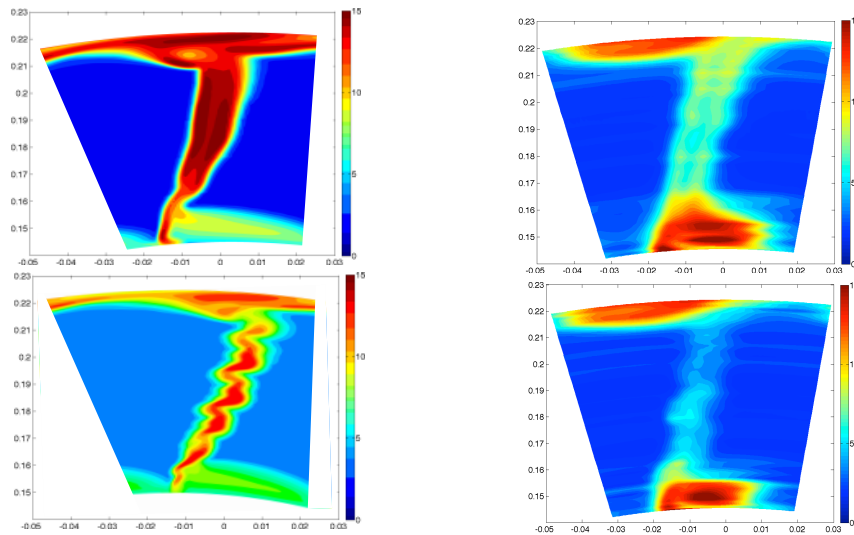


**Figure 7.** Blade channel turbulent intensity plots provided by RANS-SST (left) and experiment (right): baseline (top) and blowing (bottom) cases

The LES simulation is useful to capture unsteady phenomena like the flow near the blowing slit plotted in Fig. 8 for the baseline and blowing cases, which reveals a strong blowing effect that tends to delay the separation and reattachment points of the boundary layer almost up to the blowing slit. LES predictions were carefully checked by comparing the relevant averaged fields to those provided by RANS at same spanwise position. Angular profiles of turbulence intensity deduced from LES (with/without blowing) at inter-stage position are plotted in Fig. 9 and compared to the RANS (k-L) baseline solution.  $T_u$  is strongly reduced by the blowing and baseline solutions are found to be rather close to experiment with an LES amplification that could be attributed to confined grid (quasi-2D) effects.

Finally, the radial profiles of  $T_u$  obtained from all CFD are compared to experiment on baseline case (Fig. 10, left), showing best agreement for the RANS-SST model. Blowing efficiency provided by USI RANS is found comparable to the measurements in terms of  $T_u$  reduction (Fig. 10, right).

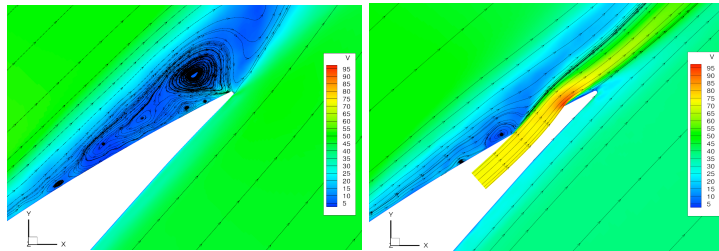


**Figure 8.** Relative velocity amplitude and streamlines near the blowing slit without (left) and with (right) blowing

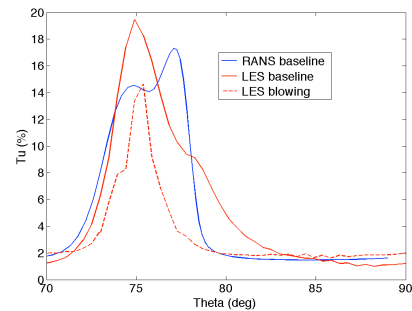


**Figure 9.** LES  $T_u$  profiles compared to RANS (k-L) baseline solution at mid-span

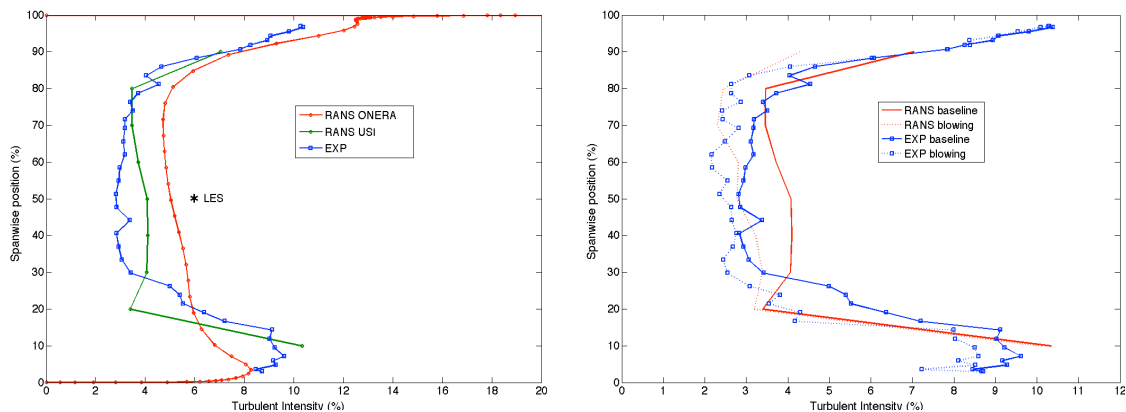


**Figure 10.**  $T_u$  radial profiles: CFD vs. experiment on baseline case (left) and blowing efficiency (right)

## 4.2 Turbulent velocity spectra and correlation scales

LES simulation data are post-processed in order to assess the turbulent velocity spectra and correlation scales. PSD of upwash velocity component ( $S_{u_{rms}}$  in Eq. (4)) calculated at inter-stage for baseline and blowing cases are compared in Fig. 11 to the Von-Karman spectra (used in Eq. (3)). Slopes are similar, but a hump over a wide frequency range can be observed in the LES solutions. The streamwise 0-time shift cross-correlation function (applied to the streamwise velocity component) is compared for baseline case to the theoretical Gaussian solution<sup>10</sup> in Fig. 12 left, showing a very good agreement. The integral scale  $\Lambda$  (deduced by integration over  $x$ ) is found to be close (at mid-span) to the RANS-based solutions plotted Fig. 12 right. Turbulent (streamwise) velocity spectra measured by hot-wire probes at 74% and 44% span are plotted in Fig. 13 left and right, respectively. These are compared to the LES solution scaled in level (-10 dB) and overplotted in Fig. 13 left, showing very close attenuation slopes and similar trends of blowing effects at 74%. However, blowing at 44% is no more efficient with a level increase for frequencies beyond 4 kHz.

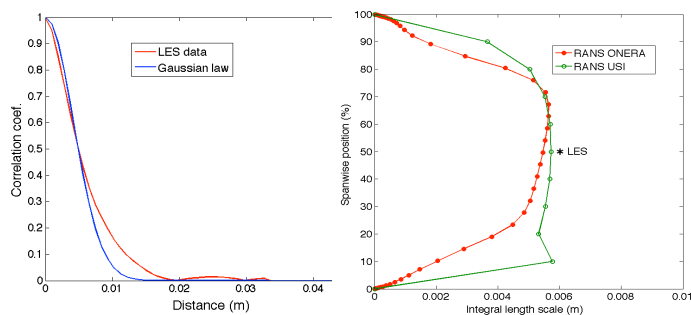
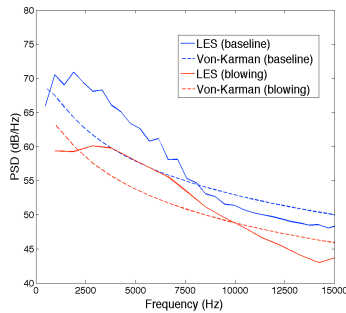


**Figure 11.** PSD of upwash turbulent velocity issued from LES and Von-Karman model **Figure 12.** LES-based streamwise correlation function (left) and integral length scales deduced from RANS and LES (right)

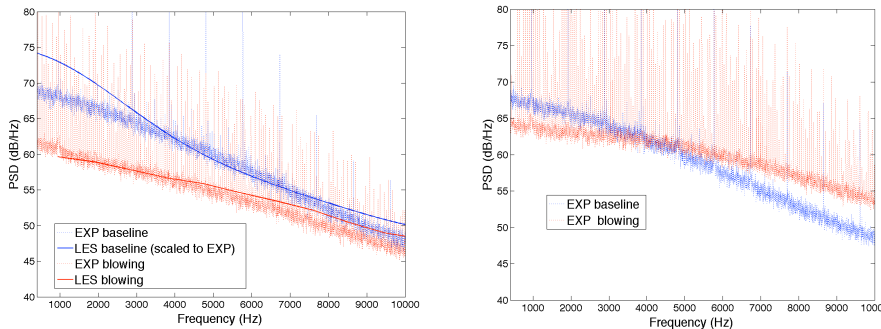


**Figure 13.** PSD of streamwise turbulent velocity at 74% span (left) and at 44% span (right)

## 4.3 Assessment of sound power level broadband noise reduction

Previous RANS and LES analyses are used to estimate the acoustic pressure PSD in the outlet duct (outer wall), as shown in Fig. 13 for the baseline case. The LES-based prediction is achieved by applying a basic scaling correction  $10 \log(L_{span} / L_{strip})$  on the SPL. A satisfactory agreement is obtained for the RANS-based solutions, whereas the LES-based spectrum is over-predicted (certainly due to the quasi-2D approach restrictions). However, the frequency slope using LES seems better appraised. Finally, broadband noise power level (PWL) spectra using RANS-SST and LES input data are presented and compared to the experiment (SPL spectra) in Fig. 14 left and right, respectively. As expected from turbulent wake analyses, significant reductions are observed in the computation results with relative level attenuations that are twice for LES compared to RANS (about 7 dB vs. 3.5 dB max), but with quite similar behavior with respect to frequency. Unfortunately, experimental results do not display any noise reduction, neither for the tones (see the non-filtered spectra), and even more highlight a broadband level increase for frequencies beyond 4 kHz (as already observed in Fig. 13 right). This is disappointing since the hot-wire measurements showed important reduction of velocity defect and turbulent wakes. Non-homogeneous wake filling from blade-to-blade as well as blowing self jet noise might explain this test failure.

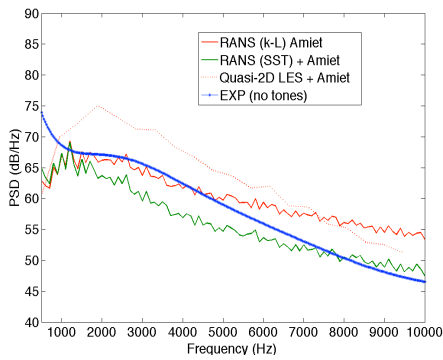


**Figure 14.** PSD baseline comparisons issued from calculations and experiment

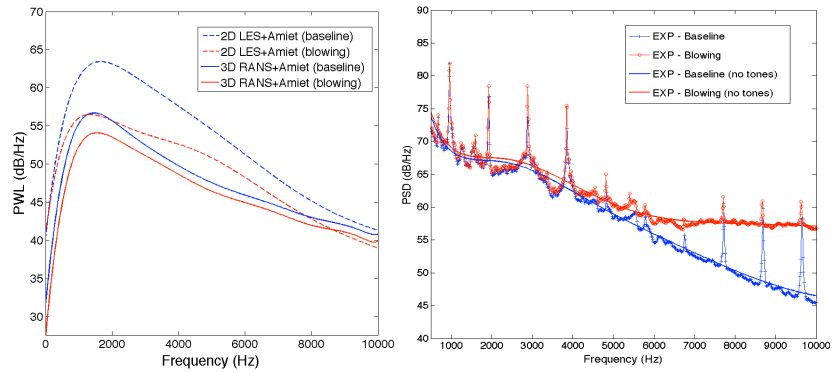


**Figure 15.** Blowing effect on broadband noise spectra: PWL predictions (left) and SPL measurements (right)

## 5. Conclusions

A comprehensive study of turbofan broadband noise reduction using a trailing edge blowing device has been carried out numerically and experimentally in a laboratory axial compressor stage rig. The blowing design and optimal settings were obtained through extensive RANS computational studies. 3D RANS simulations have been supplemented by quasi-2D LES in order to better assess the turbulent characteristics of the flow, and CFD post-processed data have been used as input to an Amiet-based acoustic calculation. Wake analyses have shown relevant reductions of velocity defect and turbulent intensity, in good agreement with the hot-wire measurements performed in the inter-stage plane. These are responsible for significant SPL attenuations in the outlet duct spectra (up to 3.5 dB for RANS-based and up to 7 dB for LES-based solutions) with a similar response to frequency, which lets the present methodology appear reliable. However, the acoustic measurements have not revealed any acoustic performance of the blowing (even more some noise increase was detected at high frequencies). This mismatch is attributed to a non-homogeneous wake filling from blade-to-blade due to small variations of geometry and to possible jet noise emitted from the slits (not considered in the simulations).

**Acknowledgements.** This work was supported by European Commission (FLOCON).

## REFERENCES

- <sup>1</sup> Brookfield, J. M., Waitz, I. A, *Trailing-Edge Blowing for Reduction of Turbomachinery Fan Noise*, Journal of Propulsion and Power, Vol. 16, No. 1, pp. 57-64, 2000.
- <sup>2</sup> Sutliff, D. L., Tweedt, D. L., Fite, E. B., and Envia, E., *Low Speed Fan Noise Reduction with Trailing Edge Blowing*, NASA/TM-2002-211559, 2002.
- <sup>3</sup> Sutliff, D. L., *Broadband Noise Reduction of a Low-Speed Fan Noise Using Trailing Edge Blowing*, NASA/TM-2005-213814 and AIAA-2005-3028, 2005.
- <sup>4</sup> Kohlhaas, M., Carolus, T., *Trailing Edge Blowing for Reduction of Rotor-Stator Interaction Noise: Criteria, Design and Measurements*, ISROMAC-14, Honolulu (USA), 2012.
- <sup>5</sup> Ansys, *Ansys CFX-Solver, Release 10.0: Modelling*, Canonsburg, Pennsylvania., 2005.
- <sup>6</sup> Riou, J., Léwy, S. and Heib, S., *Large Eddy Simulation for predicting rotor-stator broadband interaction fan noise*, Inter-Noise 2007, Istanbul, August 2007.
- <sup>7</sup> Ashcroft G., Nurnberger, D., *A computational investigation of broadband noise generation in a low-speed axial fan*, AIAA-2009-3219, Miami (Florida), 2009.
- <sup>8</sup> Nicoud, F., Ducors, F., *Subgrid-scale stress modelling based on the square of the velocity gradient*, Flow Turbulence and Combustion, Vol. 62(3), pp. 183-200, 1999.
- <sup>9</sup> Reboul, G., Polacsek, C., Léwy, S. and Heib, S., *Ducted-fan Broadband Noise Simulations Using Unsteady or Averaged Data*, Inter-noise2008, Shanghai (China), 2008.
- <sup>10</sup> Lynch, D.A., Mueller, T.J., and Blake, W.K., *A Correlation Length Scale for the Prediction of Aeroacoustic Response*, AIAA-2002-2569, 2002.